PROCEEDINGS OF SCIENCE

Precision Predictions for Polarized Electroweak Bosons

Rene Poncelet[a,*]

[a] *Institute of Nuclear Physics,*
ul. Radzikowskiego 152, 31–342 Krakow, Poland

E-mail: rene.poncelet@ifj.edu.pl

The Higgs boson discovery at the Large Hadron Collider (LHC) completed the Standard Model of Particle Physics, and it confirmed the Higgs mechanism as a suitable description of the Electroweak- Symmetry-Breaking (EWSB). Nevertheless, the dynamics of the EWSB is still one of the most consequential questions in particle physics and a fascinating topic due to its connection to other open questions about the structure of the early universe, matter-anti-matter asymmetry and fermionic mass hierarchies. A pathway to study the EWSB mechanism is to investigate the longitudinal polarisation state of massive electroweak bosons. In this presentation, I will discuss the computation and phenomenology of higher-order QCD effects on polarised boson production cross-sections at the LHC and their impact on extracting the longitudinal polarisation fractions.

42nd International Conference on High Energy Physics (ICHEP2024)
18-24 July 2024
Prague, Czech Republic

*Speaker

PoS(ICHEP2024)395

Introduction. One of the most remarkable feats of the Standard Model of Particle Physics was the predictions and discovery of the Higgs boson. While this success has tremendous implications for how physics at colliders like the Large Hadron Collider (LHC) is perceived today, the exact mechanism behind electroweak symmetry breaking (EWSB) is still elusive. Measurements of the Higgs self-interactions will show whether the Higgs potential, as postulated in the SM, is realised in nature. An alternative approach to investigate the EWSB is to focus on the Goldstone bosons or, phrased differently, on the longitudinal polarisation states of the masses of Electroweak (EW) gauge bosons. These longitudinal modes and their interactions are ultimately constrained through the SM, giving a unique opportunity to stress test the SM. The EW bosons have only a limited lifetime, and therefore, the polarisation of these bosons is not directly accessible experimentally. However, thanks to the electroweak interactions vector and axial-vector coupling structure, it is possible to obtain sensitivity to the boson polarisation state from angular distributions of their decay products.

Providing accurate and precise theory predictions for polarised boson production cross-section has become an active field of research. The research has been driven by the insight that higher-order QCD and EW effects impact the polarisation fraction, i.e. the fraction of events with a given boson polarisation. Thus, their inclusion is crucial to achieving reliable extraction from experimental data. The state-of-the-art for producing a single or a pair of bosons and vector boson scattering are QCD and Electroweak (EW) next-to-leading order corrections, possibly matched to parton-showers [1–9]. In a few cases, second-order QCD cases have been computed [10–12].

This article highlights some of the results from second-order QCD corrections and their implications. Also, it presents the first steps to include polarisation-dependent cross-sections within the HighTEA framework [14] to facilitate the use of these higher-order calculations in phenomenology.

Predictions for polarized boson production. The article focuses on the production of one or more electroweak boson(s) in their decay into leptons. Considering the matrix elements contributing to these processes, the intermediate propagating bosons are generally unpolarised. The contributions of individual polarisation states can access in the on-shell limit of the bosons (technically, this can be achieved in the Narrow Width Approximation or Pole-approximation) through the decomposition of the numerator of the boson-propagator(s) into a sum over polarisation vectors, i.e., $\left(-g^{\mu\nu} + k^\mu k^\nu/k^2\right) \to \sum_\lambda \epsilon_\lambda^{*\mu}\epsilon_\lambda^\nu$. Propagating such decomposition to the matrix element which eventually enters the cross-section we achieve a separation into matrix elements of specified polarisation λ and interference terms: $|M|^2 = \sum_\lambda |M_\lambda|^2 + \sum_{\lambda\neq\lambda'} M_\lambda^* M_{\lambda'}$. In this way, we can write the physical cross-section as a decomposition of polarised components:

$$\frac{\mathrm{d}\sigma}{\mathrm{d}X} = f_T\frac{\mathrm{d}\sigma_T}{\mathrm{d}X} + f_L\frac{\mathrm{d}\sigma_L}{\mathrm{d}X}\left(+f_{int.}\frac{\mathrm{d}\sigma_{int.}}{\mathrm{d}X}\right) ,$$

where we kept the left and right transverse components in a coherent transverse polarisation state. This decomposition generalises to more than one polarised boson. In the above normalisation, the polarisation fractions f_i are "predicted" to be unity by the Standard Model. Considering the polarised cross sections as templates and fitting their coefficients f_i to data can be considered a test of the Standard Model and probes BSM physics. Crucially, it has been noticed that the fractions receive substantial corrections from real and virtual contributions entering at higher order QCD

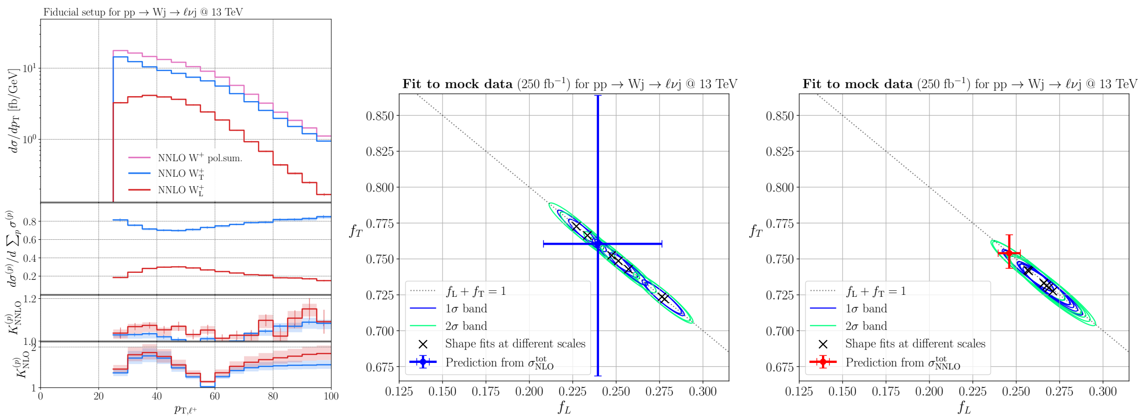

Figure 1: Selected results from ref. [11] for $W + j$ production. On the left: polarized differential distributions w.r.t to $p_T(e^+)$. Middle and right: mock-data fits to extract the polarization fractions from differential distributions. See the main text for more details.

and EW computations and, therefore, motivate their computation and detailed assessment of the uncertainties entering the theoretical computations of such polarised templates.

Phenomenology of higher-order QCD corrections. This section highlights the impact of second-order QCD corrections on polarisation fractions in the $W + j$ production [11, 12] processes. A first observation is the significance of second-order QCD corrections. On the left-hand side of figure 1, we show for the W^+j final state the differential distribution concerning the transverse momentum of the positron $p_T(e^+)$. The top panel shows the absolute distribution for the transverse T and longitudinally L polarised W boson and the sum of the two contributions, neglecting interference terms. The differential polarisation fraction is visualised in the second panel, followed by the differential NLO and NNLO QCD k-factors for the individual polarised cross sections, respectively. Besides the typical NNLO QCD effect of reduced perturbative corrections and scale dependence, it is important to note that the two polarisation states receive different higher-order corrections, which imply changes in the differential polarisation fractions. These differences imply that a fit requires including these higher-order terms to avoid biases. Similar observations have been made in the context of W^+W^- production [10]. The former point is further demonstrated on the middle and right side of figure 1, which shows a simplified mock-data fit (generated from off-shell NNLO QCD theory assuming 250 fb^{-1} luminosity) using NLO and NNLO QCD theory. We direct the reader to ref. [11] for details of the fit. The coloured cross shows the SM prediction of the polarisation fraction and the respective scale dependence. The individual ellipses are fits obtained for different scale choices (the same that go into the scale bands); they are lined up along the diagonal due to the constraint $f_T + f_L = 1$ that is imposed. One sees that the NLO results have a much wider spread than those including the NNLO QCD corrections.

Polarisation studies in HighTEA. While NNLO (and even higher order) QCD predictions have become a crucial pillar of LHC precision phenomenology, public numerical codes are still relatively rare. In the context of polarised cross sections, the only results have been produced within a private implementation of the sector-improved residue subtraction scheme [13]. The HighTEA framework

[14] has been designed to provide access to results in a flexible, easy-to-use and efficient manner. The extension of this framework to include polarisation information is a work in progress [1].

Acknowledgement. RP acknowledges the support from the COMETA COST action (CA22130).

References

[1] A. Denner and G. Pelliccioli, JHEP **09**, 164 (2020) doi:10.1007/JHEP09(2020)164 [arXiv:2006.14867 [hep-ph]].

[2] A. Denner and G. Pelliccioli, Phys. Lett. B **814**, 136107 (2021) doi:10.1016/j.physletb.2021.136107 [arXiv:2010.07149 [hep-ph]].

[3] A. Denner and G. Pelliccioli, JHEP **10**, 097 (2021) doi:10.1007/JHEP10(2021)097 [arXiv:2107.06579 [hep-ph]].

[4] D. N. Le and J. Baglio, Eur. Phys. J. C **82**, no.10, 917 (2022) doi:10.1140/epjc/s10052-022-10887-9 [arXiv:2203.01470 [hep-ph]].

[5] D. N. Le, J. Baglio and T. N. Dao, Eur. Phys. J. C **82**, no.12, 1103 (2022) doi:10.1140/epjc/s10052-022-11032-2 [arXiv:2208.09232 [hep-ph]].

[6] M. Hoppe, M. Schönherr and F. Siegert, JHEP **04**, 001 (2024) doi:10.1007/JHEP04(2024)001 [arXiv:2310.14803 [hep-ph]].

[7] G. Pelliccioli and G. Zanderighi, Eur. Phys. J. C **84**, no.1, 16 (2024) doi:10.1140/epjc/s10052-023-12347-4 [arXiv:2311.05220 [hep-ph]].

[8] A. Denner, C. Haitz and G. Pelliccioli, Phys. Lett. B **850**, 138539 (2024) doi:10.1016/j.physletb.2024.138539 [arXiv:2311.16031 [hep-ph]].

[9] T. N. Dao and D. N. Le, Eur. Phys. J. C **84**, no.3, 244 (2024) doi:10.1140/epjc/s10052-024-12579-y [arXiv:2311.17027 [hep-ph]].

[10] R. Poncelet and A. Popescu, JHEP **07**, 023 (2021) doi:10.1007/JHEP07(2021)023 [arXiv:2102.13583 [hep-ph]].

[11] M. Pellen, R. Poncelet and A. Popescu, JHEP **02**, 160 (2022) doi:10.1007/JHEP02(2022)160 [arXiv:2109.14336 [hep-ph]].

[12] M. Pellen, R. Poncelet, A. Popescu and T. Vitos, Eur. Phys. J. C **82**, no.8, 693 (2022) doi:10.1140/epjc/s10052-022-10641-1 [arXiv:2204.12394 [hep-ph]].

[13] M. Czakon and D. Heymes, Nucl. Phys. B **890**, 152-227 (2014) doi:10.1016/j.nuclphysb.2014.11.006 [arXiv:1408.2500 [hep-ph]].

[14] M. Czakon, Z. Kassabov, A. Mitov, R. Poncelet and A. Popescu, [arXiv:2304.05993 [hep-ph]].

[1] An example is available here: `https://www.precision.hep.phy.cam.ac.uk/hightea/`